



The effect of the equatorial Pacific cold SST bias on simulated ENSO teleconnections to the North Pacific and California

Tobias Bayr¹ · Daniela I. V. Domeisen² · Christian Wengel¹

Received: 21 September 2018 / Accepted: 25 March 2019 / Published online: 3 April 2019
© Springer-Verlag GmbH Germany, part of Springer Nature 2019

Abstract

Precipitation in California is modulated by variability in the tropical Pacific associated with El Niño/Southern Oscillation (ENSO): more rainfall is expected during El Niño episodes, and reduced rainfall during La Niña. It has been suggested that besides the shape and location of the sea surface temperature (SST) anomaly this remote connection depends on the strength and location of the atmospheric convection response in the tropical Pacific. Here we show in a perturbed physics ensemble of the Kiel Climate Model and CMIP5 models that due to a cold equatorial SST bias many climate models are in a La Niña-like mean state, resulting in a too westward position of the rising branch of the Pacific Walker Circulation. This in turn results in a convective response along the equator during ENSO events that is too far west in comparison to observations. This effect of the equatorial cold SST bias is not restricted to the tropics, moreover it leads to a too westward SLP response in the North Pacific and too westward precipitation response that does not reach California. Further we show that climate models with a reduced equatorial cold SST bias have a more realistic representation of the spatial asymmetry of the teleconnections between El Niño and La Niña.

Keywords El Niño/Southern Oscillation · Sea surface temperature bias · North Pacific teleconnections · Rainfall over California · Perturbed physics ensemble · CMIP5

1 Introduction

El Niño Southern Oscillation (ENSO) accounts for the dominant part of interannual variability in the tropical Pacific with significant and disrupting impacts on the global atmospheric and oceanic circulation (e.g. Trenberth et al. 1998). Remote impacts of ENSO include its influence on winter precipitation over the North American west coast (Piechota and Dracup 1996; Yoon and Leung 2015; Jong et al. 2016; Kumar and Chen 2017; Dong et al. 2018). In particular, the connection between ENSO and precipitation in California has been studied using both observations and models (e.g. Schonher and Nicholson 1989; Mo and Higgins 1998), as the agricultural sector is strongly dependent on rainfall in this already drought-prone region (MacDonald et al. 2008).

Californian rainfall tends to be above-average during El Niño events (e.g. Piechota et al. 1997; Cayan et al. 1999), and especially Southern California is strongly affected by this teleconnection (Jong et al. 2016; Hoell et al. 2016). The El Niño teleconnection is characterized by a Rossby wave train (e.g. Hoskins and Karoly 1981) triggered by anomalous tropical heating and convection. This anomaly induces a positive phase of the Pacific-North American pattern (PNA) (Wallace and Gutzler 1981; Leathers et al. 1991; Leathers and Palecki 1992), characterized by a strengthened Aleutian low (Mo and Livezey 1986; Barnston and Livezey 1987), a positive pressure anomaly over western Canada, and a negative anomaly over the south-eastern United States, accompanied by a southward shift of the storm track (Seager et al. 2010). These impacts on the North Pacific region tend to be reversed for La Niña years.

The link between ENSO and rainfall in California however exhibits asymmetries between El Niño and La Niña events (e.g. Zhang et al. 2014) as well as non-stationarity (Rasmusson and Wallace 1983), i.e., not every El Niño winter tends to be wet in California, such as the dry El Niño winter 2015/16 (Paek et al. 2017; Wang et al. 2017; Siler

✉ Tobias Bayr
tbayr@geomar.de

¹ GEOMAR Helmholtz Centre for Ocean Research,
Düsternbrooker Weg 20, 24105 Kiel, Germany

² Institute for Atmospheric and Climate Science, ETH Zürich,
Switzerland

et al. 2017; Zhang et al. 2018a). The impact in the North Pacific region strongly depends on the nature of the forcing in the tropical Pacific (Frauen et al. 2014; Hoell et al. 2016; Jiménez-Estève and Domeisen 2019), such as the strength and the location of the sea surface temperature (SST) anomaly in the equatorial Pacific: Central Pacific (CP) El Niño, also called Modoki El Niño (Ashok et al. 2007; Capotondi et al. 2015), differs in its teleconnections from East Pacific (EP) El Niño peaking in the eastern equatorial Pacific (Larkin and Harrison 2005; Hurwitz et al. 2011; Garfinkel et al. 2012b). For example CP El Niño events are more related with extreme precipitation over California by the PNA teleconnection, while EP El Niño events are more related with non-extreme precipitation by the North Pacific Oscillation teleconnection (Chen et al. 2018; Dong et al. 2018). Over the past decade CP El Niño events have become more prominent (McPhaden 2012; Guan and McPhaden 2016). A considerably weaker distinction according to the peak location of the SST anomalies is found among La Niña events (Kug and Ham 2011; Ding et al. 2017).

The location of the SST anomaly influences the location of the convective response along the equator, which in turn affects the location of the sea level pressure (SLP) response in the North Pacific (Ding et al. 2017), although the strength of the tropical anomaly alone can also affect the location of the North Pacific anomaly (Jiménez-Estève and Domeisen 2019). During El Niño (La Niña) events the positive (negative) SST anomalies act as a heat source (sink) in the tropics and can trigger atmospheric Rossby waves that transport the signal to the extratropics (Gill 1980). Due to different atmospheric mean states the resulting teleconnections can be quite distinct even under similar SST anomalies (Ding et al. 2017). In fact, recent observational studies suggest that ENSO teleconnections depend more strongly on the location and strength of the anomalous convection at the equator as compared to the SST anomaly (Chiodi and Harrison 2013, 2015; Ding et al. 2017). It is however important to note that due to the limited observational record of ENSO events the teleconnections contain significant uncertainty with regard to the origin of differences in the teleconnections, which might be linked to the asymmetry between El Niño and La Niña and the nonlinearity between different El Niño flavors, but also to changes in the background state that the teleconnections encounter (Deser et al. 2017, 2018; Garfinkel et al. 2018; Domeisen et al. 2019).

Despite considerable progress over the past decades in understanding the mean state and variability in the tropical Pacific, current climate models still exhibit shortcomings in this region (e.g. Bellenger et al. 2014; Timmermann et al. 2018): Many state-of-the-art climate models exhibit a cold SST bias in the equatorial Pacific, leading to a more La Niña-like mean state with the rising branch of the Walker Circulation located too far west, causing a weaker

and further westward convective response during El Niño as compared to observations (Latif and Keenlyside 2009; Kug and Ham 2011; Kim and Cai 2014; Bayr et al. 2014; Domeisen et al. 2015; Bayr et al. 2018a). Further the cold SST bias leads to an underestimated positive zonal wind feedback and the negative net surface heat flux feedback in most models participating in the Coupled Model Intercomparison Project phase 5 (CMIP5), as both are strongly linked to the convective response along the equator (Lloyd et al. 2012; Bellenger et al. 2014; Bayr et al. 2018a). These problems hamper simulated ENSO dynamics in climate models (Dommenget et al. 2014; Bayr et al. 2018b), weakens the seasonal phase locking (Wengel et al. 2018), the asymmetry between El Niño and La Niña (Bayr et al. 2018a) and the asymmetry between CP and EP events (Sun et al. 2016). The correct simulation of the location, timing, and strength of ENSO in models is however crucial for predicting the induced teleconnections and potential asymmetries between events that has been suggested to lead to nonlinear behavior in teleconnections (Frauen et al. 2014; Garfinkel et al. 2018; Domeisen et al. 2019).

While the influence of the cold bias on the location of the convective response at the equator is quite well understood (Bayr et al. 2018a), it remains an open question to which extent SST biases impact ENSO teleconnections. We therefore address in this study the impact of an equatorial Pacific SST bias on the North Pacific atmospheric teleconnection, with a focus on California. We analyze a perturbed physics ensemble of the Kiel Climate Model (KCM) that has a similar spread in equatorial SST bias as observed in the CMIP5 models. Section 2 introduces the model and observational data, Sect. 3 investigates the relation between the equatorial Pacific SST bias and the position of the rising branch of the Pacific Walker Circulation in the KCM. In Sect. 4 we show the influence of the equatorial cold SST bias on the equatorial convective response and in Sect. 5 the influence on the teleconnection to the North Pacific. In Sect. 6 we perform a similar analysis for a CMIP5 ensemble and Sect. 7 offers a discussion of the results.

2 Data and methods

Model simulations are performed with a global coupled general circulation model, the Kiel Climate Model (KCM, Park et al. 2009), which consists of the ECHAM5 atmospheric general circulation model (Roeckner et al. 2003) and the NEMO ocean general circulation model (Madec 2008). The atmosphere has a T42 horizontal resolution ($2.8^\circ \times 2.8^\circ$) and 19 vertical layers and the Ocean an orca2 grid with 31 vertical levels. We use here a perturbed physics ensemble of 28 experiments, in which we change the convection parameters to generate different mean states and SST biases. We

change the “convective cloud conversion rate from cloud water to rain”, “entrainment rate for shallow convection” and “convective mass-flux above level of non-buoyancy”, which are also used to tune the climate models and are described in detail in Mauritsen et al. (2012). We use the same experiments as Wengel et al. (2018) and the experiments are described there more in detail. Varying the convection parameters yields a spread in the equatorial Pacific SST bias that is comparable to the multi-model ensemble of CMIP5 (Wengel et al. 2018; Bayr et al. 2018a). To demonstrate how the KCM performs with unbiased SSTs, we analyze a set of eight atmosphere-only experiments (hereafter: AMIP-type) driven by observed daily SSTs from NOAA OISST data (Banzon et al. 2016) for the period 1982–2016. The AMIP-type experiments all have standard convection parameters and only differ in the initial conditions.

Further we use the historical experiment (1900–1999) of the CMIP5 data base (Taylor et al. 2012). All models are used for which all required variables were available (see Fig. 11b for a list of the models used in this study). The CMIP5 data is interpolated onto a regular $2.5^\circ \times 2.5^\circ$ grid.

For comparison of the model results, the following datasets are used for the period 1979–2016: SST observations from the NOAA OISST data (Banzon et al. 2016), outgoing longwave radiation (OLR) from NOAA (Liebmann and Smith 1996), precipitation from CMAP (Xie and Arkin 1997), SLP from ERA-Interim reanalysis (Dee et al. 2011). We focus here on the boreal winter season (DJFM), when the ENSO teleconnection to the North Pacific is strongest. The number of months available for the analysis for each dataset is indicated in the figure headers.

Due to the changed convection parameters in the perturbed physics ensemble of the KCM, the global mean temperature shows a considerable spread in the KCM experiments from observed global mean temperature (up to $\pm 2\text{K}$). But also the CMIP5 experiments show a spread of $\pm 1\text{K}$ from observed global mean temperature. Therefore the minimum temperature threshold for convection in the tropics, as suggested by e.g. Tompkins (1997), Wang et al. (2011), Chiodi and Harrison (2013), Chiodi and Harrison (2015) and Johnson and Kosaka (2016), will be shifted in the different experiments, as described by Bayr and Dommenget (2013). To account for this shift in the convection threshold, we here use the relative temperature in the tropics, i.e. we subtract the area mean SST over the tropical Pacific (120°E – 70°W , 30°S – 30°N) from each data set before computing the SST bias. Based on the SST bias strength in the Niño4 region, three sub-ensembles of KCM experiments are defined, termed SMALL ($> -0.4\text{K}$), LARGE ($< -0.9\text{K}$) and MEDIUM (between SMALL and LARGE). Choosing other regions for defining the relative SST bias (e.g. the entire tropics or the tropical Pacific from 15°S to 15°N) has only a very limited influence on which sub-ensemble each experiment is contained in. We select our sub-ensembles on

the basis of the SST bias in the Niño4 region, as it strongly determines the position of the rising branch of the Pacific Walker Circulation (Bayr et al. 2018a).

ENSO events are defined based on Trenberth (1997): an El Niño (La Niña) event occurs if the 5-month running mean Niño3.4 SST is above +1 (below -1) standard deviation for at least 6 consecutive months. An EP (CP) El Niño is defined by a positive (negative) Trans Niño Index (TNI, Trenberth and Stepaniak 2001), which is the difference between Niño1.2 SST and Niño4 SST, after normalizing each by its standard deviation. No distinction with respect to EP vs CP La Niña is made due to the smaller difference.

The center of heat index (CHI, Giese and Ray 2011) is used for the detection of the longitude and amplitude of the ENSO patterns. The CHI longitude is the amplitude-weighted center of mass of the SST pattern along the equator between 5°S and 5°N , i.e. the average over all amplitude-weighted longitudes that exceed 0.5 standard deviations of the Niño3.4 index. The CHI amplitude is the average amplitude over all grid points that exceed 0.5 standard deviations of the Niño3.4 index. The same method is applied to detect the longitude and amplitude of the OLR anomaly along the equator, using the mean standard deviation of OLR in Niño4 as a threshold, SLP between 30°N and 70°N , using the mean standard deviation of SLP in that area as a threshold, and precipitation between 30°N and 45°N , using the mean standard deviation of precipitation in this area as a threshold. Significance of the composites is tested using a bootstrapping approach. For a better comparison, all composite plots except for SST are normalized by the amplitude of the CHI index of SST.

We use the horizontal wave-activity flux to highlight the propagation features of quasi-stationary Rossby waves and the associated teleconnection patterns according to Takaya and Nakamura (2001) and Ding et al. (2017):

$$W = \frac{1}{2|\bar{U}|} \left[\bar{u}(\Psi_x'^2 - \Psi' \Psi_{xx}') + \bar{v}(\Psi_x' \Psi_y' - \Psi' \Psi_{xy}') \right] \quad (1)$$

$$\left[\bar{u}(\Psi_x' \Psi_y' - \Psi' \Psi_{xy}') + \bar{v}(\Psi_y'^2 - \Psi' \Psi_{yy}') \right]$$

here Ψ' , u and v denote the perturbations of the geostrophic streamfunction, the zonal and meridional wind, respectively. The overbar represents the basic state or climatological mean. The subscripts x and y indicate the partial derivatives in the zonal and meridional directions, respectively.

3 SST biases and atmospheric mean state

State-of-the-art climate models still exhibit considerable SST biases (Fig. 1a), especially where the SST gradients are large, as e.g., at the location of the western boundary currents in the North Atlantic (Drews et al. 2015), or where

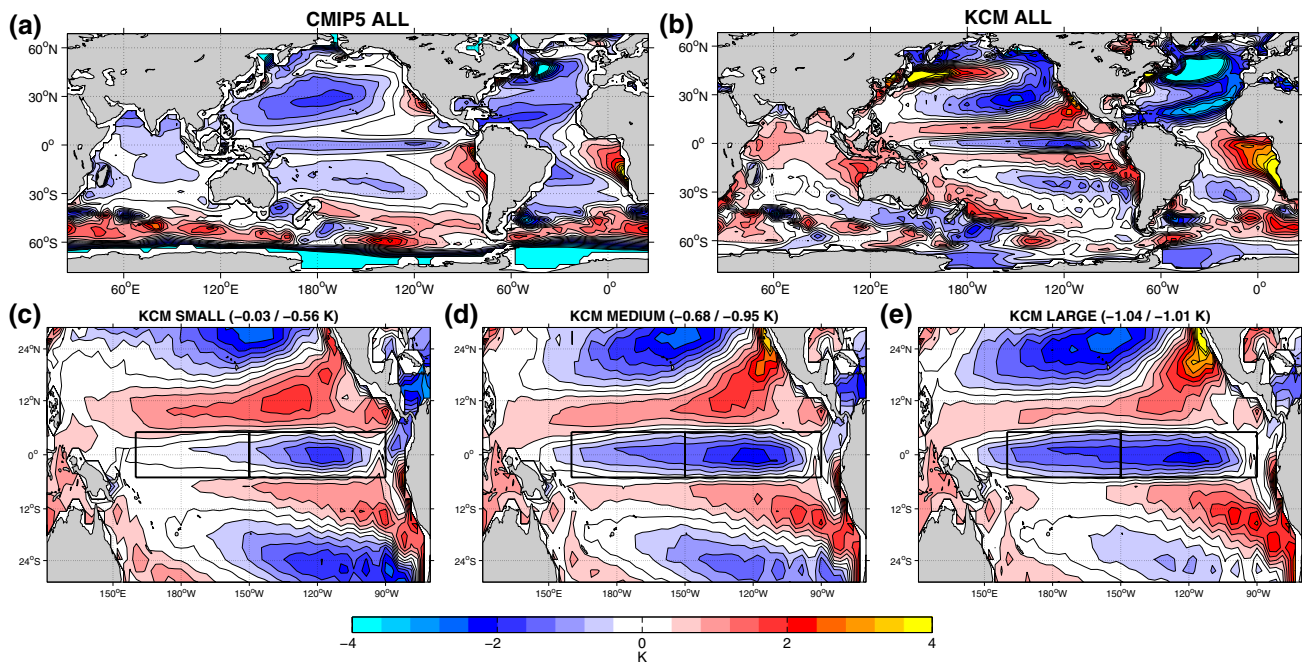


Fig. 1 Relative SST bias in comparison to NOAA OISST in **a** for CMIP5 ensemble (i.e. global mean SST is subtracted from each data set before calculating the SST bias), in **b** same as **a**, but here for all KCM experiments, in **c** the tropical SST bias (i.e. tropical Pacific mean SST is subtracted from each data set before calculating the SST

bias) for the SMALL SST bias sub-ensemble (nine experiments), in **d** same as **c** but here for the MEDIUM SST bias ensemble (ten experiments), in **e** same as **c**, but here for the LARGE SST bias sub-ensemble (nine experiments)

the costal upwelling is not well simulated in coarse resolution climate models, as e.g. at the eastern boundaries of the tropical Pacific and South Atlantic (Harlaß et al. 2015). The largest SST biases in the KCM are in similar regions and a bit larger in magnitude than those in the CMIP5 ensemble (Fig. 1a, b). We have to note that these two ensembles have a different SST bias in the North Pacific, as we have a warm bias in the Kuroshio region in KCM and a cold bias in CMIP5. However, as we show later in Sect. 6, despite this difference the two ensembles show a similar relationship between the equatorial SST bias and ENSO teleconnection to the North Pacific, so that we think this is of minor importance.

In the tropical Pacific the SST bias is relatively small in comparison to the aforementioned SST biases, but it has considerable impacts on ENSO dynamics, as described above. Figure 1c–e shows the SST biases in the sub-ensembles with SMALL, MEDIUM and LARGE SST biases in the equatorial Pacific, respectively. Shown is the relative SST bias, i.e. the area mean SST over the tropical Pacific (120°E–70°W, 30°S–30°N) is subtracted from each data set before calculating the SST bias. The strength of the cold bias has a considerable influence on the location of the mean convection over the western Pacific, as in the SMALL sub-ensemble the vertical motion shifts from descending to ascending at 165°W, while in the LARGE sub-ensemble

it shifts at 165°E (Fig. 2a), indicating a shift of the rising branch of the Pacific Walker Circulation by 30° to the west. There is also a strong correlation (0.96) in the individual experiments between the SST bias in the Niño4 region and the location of the shift from descending to ascending at the equator (Fig. 2b) and the strength of convection in the Niño4 region (Fig. 2c). The KCM AMIP-type experiments have the shift from ascending to descending at the same longitude as in observations, but the ascending in the western Pacific is overall too strong (Fig. 2a, c). The different mean state positions of the Walker Circulation also have a considerable impact on the two most important ENSO atmospheric feedbacks, i.e. the amplifying wind-SST feedback and the heat flux damping feedback, as shown in Fig. 3): there is a large spread in atmospheric feedbacks among the experiments (similar to the spread shown in CMIP5 models, see also Fig. 12) and a strong linear relation between the wind-SST feedback strength and heat flux-SST feedback strength (Fig. 3a). The strength of both feedbacks strongly depends on the mean state position of the rising branch of the Walker Circulation, which in turn is determined to a large extent by the equatorial SST bias (Fig. 3b), as described in Bayr et al. (2018a). Further, the underestimated ENSO atmospheric feedbacks also hamper ENSO dynamics, as described in detail in Bayr et al. (2018b), as ENSO dynamics shift from predominately wind-driven dynamics to a hybrid of

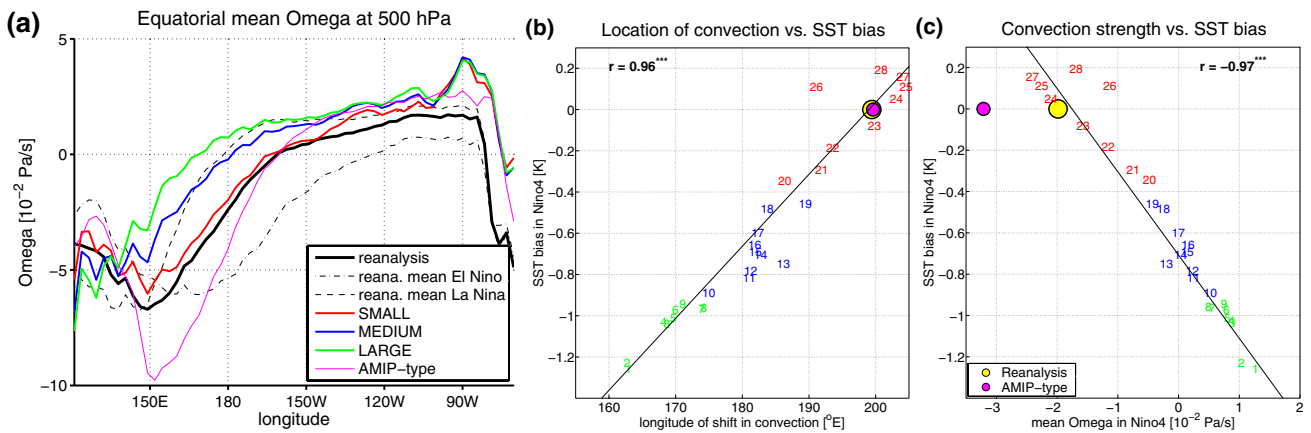
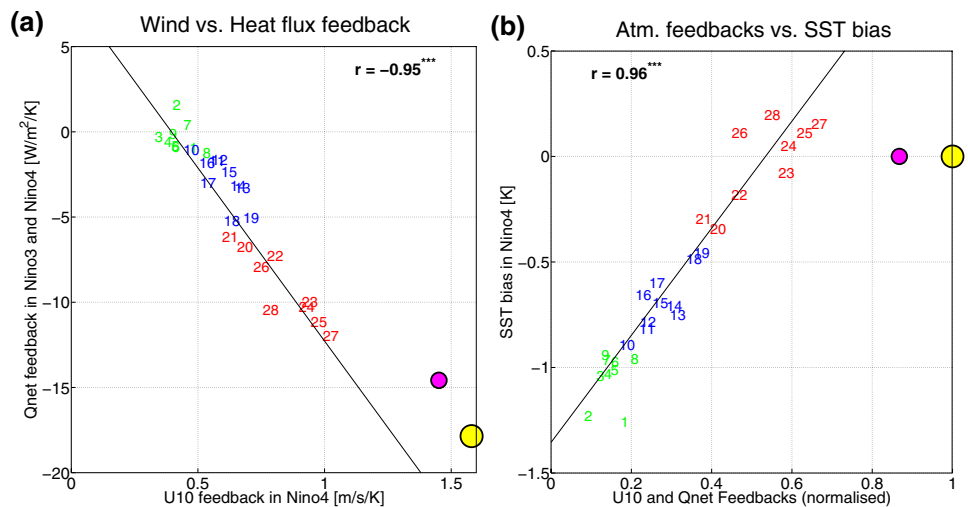


Fig. 2 **a** Equatorial mean state (5°S–5°N) of vertical wind (ω) at 500 hPa in reanalysis, in KCM sub-ensembles with SMALL, MEDIUM and LARGE SST bias and in KCM AMIP-type ensemble; The black dashed-dotted (dashed) line is the mean over all El Niño (La Niña) months in reanalysis; **b** the longitude of shift from ascending to descending in ω at 500 hPa (where ω is zero in **a**) on

the x-axis vs. the relative SST bias in Niño4, as shown in Fig. 1 on the y-axis; **c** same as **b** but here mean ω in the Niño4 region on the x-axis. The colors of the numbers in **b** and **c** indicate the sub-ensembles with SMALL, MEDIUM, LARGE SST bias. Three stars behind the correlation value indicates that the correlation is significant on a 99% confidence level

Fig. 3 **a** 10 m zonal wind-SST feedback in Niño4 on the x-axis vs. the heat flux-SST feedback in Niño3 and Niño4 region on the y-axis, **b** atmospheric feedback strength (i.e. average of wind-SST and heat flux-SST feedback, after normalizing each by the ERA-Interim value) on the x-axis vs. relative SST bias in Niño4. The colors of the numbers indicate the sub-ensembles with SMALL, MEDIUM, LARGE SST bias. Three stars behind the correlation value indicates that the correlation is significant on a 99% confidence level



wind-driven and shortwave-driven dynamics. In the following we focus on how the spread in the position of the rising branch of the Pacific Walker Circulation in the KCM affects the convective response during ENSO events at the equator and the ENSO teleconnection to the North Pacific.

4 Equatorial SST and convection response during ENSO events

The SST anomalies (SSTa) in boreal winter (DJFM) for different flavors of ENSO events (composites in Fig. 4a, b) show that the EP El Niño pattern in observations is nearly twice as strong and the center of heat lies 20° further east than for CP El Niño events (the amplitude and longitudinal

location of the center—characterized by the CHI—are indicated in the respective panel titles). La Niña is comparable in terms of shape, amplitude and center location to CP El Niño, but with a reversed sign (Fig. 4b, c). The AMIP-type simulations are forced by exactly the same data set as shown here for observations (Fig. 4a–c). In the KCM sub-ensembles with different SST biases, the difference between EP and CP El Niño is generally too weak, as the asymmetry in the pattern and amplitude is strongly underestimated (Fig. 4g–n). However, the asymmetry in amplitude is slightly better simulated in the SMALL sub-ensemble than in the LARGE sub-ensemble, as well as the number of EP and CP El Niño months. This would be expected, as the cold SST bias weakens the wind and

ENSO Composites of SST in Obs and KCM

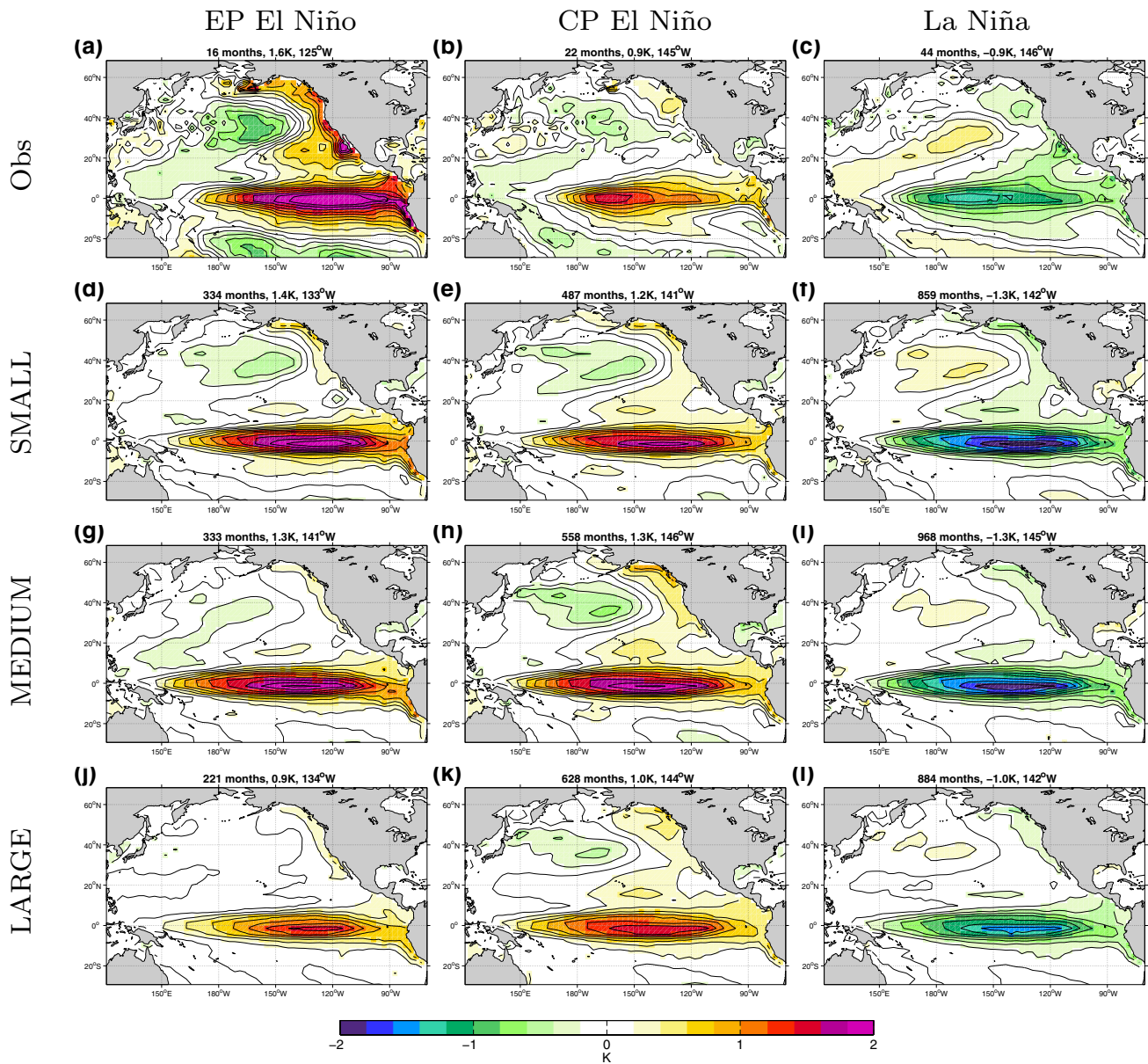


Fig. 4 SST composites for EP El Niño events, CP El Niño events and La Niña events in DJFM in **a–c** for Observations, in **d–f** for a KCM sub-ensemble with SMALL cold SST bias, in **g–i** for a KCM sub-ensemble with MEDIUM cold SST bias and in **j–l** for a KCM sub-ensemble with LARGE cold SST bias. The number in the header of

each figure is the number of months, the center of heat amplitude and center of heat longitude, respectively. Shading indicates the areas that are statistically different from zero on a 95% confidence level. See Sect. 2 for the details how the center and amplitude of the center of heat index (CHI) is calculated

thermocline feedback, thereby weakening the difference between EP and CP El Niño events (Sun et al. 2016).

As a proxy for convection and cloudiness we consider outgoing longwave radiation (OLR, Fig. 5), where negative OLR anomalies indicate anomalously strong convection. For observations, CP El Niño and La Niña again yield comparable results in terms of the longitude of the center, but the

OLR amplitude is weaker for La Niña (Fig. 5b, c). The OLR amplitude for EP El Niño is similar to CP El Niño (Fig. 5a, b), but the center is shifted eastward by 32° in comparison to CP El Niño. As the minimum temperature threshold for convection can be reached in the eastern equatorial Pacific during EP El Niño events (Johnson and Kosaka 2016), the inter-tropical convergence zone can shift southward during

strong EP El Niño events (Kao and Yu 2009), explaining the more eastward center of convection. The AMIP-type experiments are in general able to reproduce the observed OLR behavior, but with overall stronger amplitudes and too weak convective response in the equatorial eastern Pacific in the EP El Niño (Fig. 5d–f). In the coupled experiments, the OLR magnitude decreases and the center of convection experiences a considerable shift to the west from SMALL to LARGE for all three types of ENSO events (Fig. 5g–o). This can be explained by the too western position of the rising branch of the Walker Circulation in the presence of a large equatorial cold bias, as shown in Fig. 2b. Further, the spatial asymmetry between CP and EP El Niño is strongly underestimated in the coupled model, more in LARGE than in SMALL, as the difference at the center of convection is $+7^\circ$, $+1^\circ$ and -3° in LARGE, MEDIUM and SMALL, respectively, in comparison to $+32^\circ$ in observations.

5 ENSO teleconnection to the North Pacific

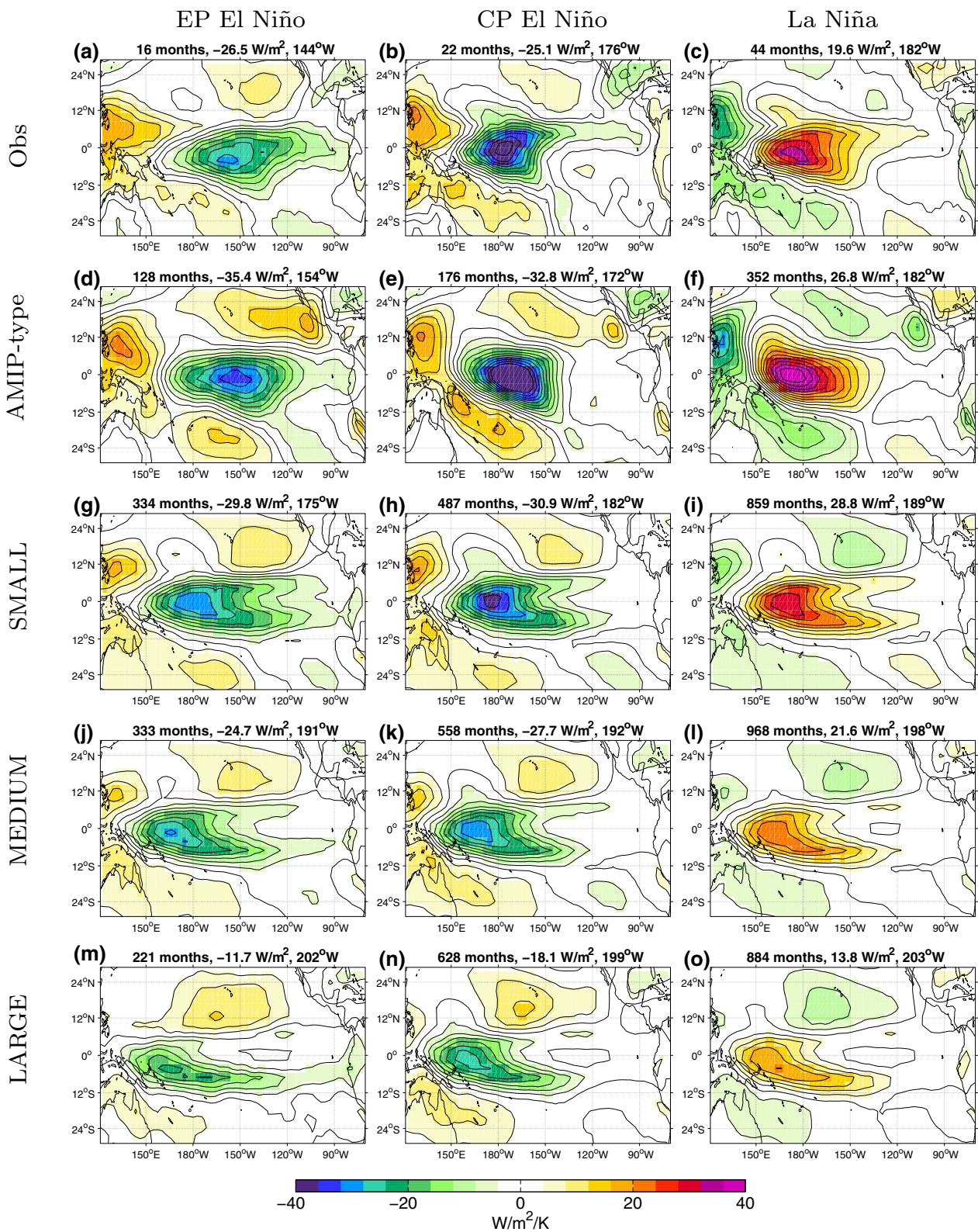
A representation of the North Pacific teleconnections for different ENSO flavors is given by the boreal winter SLP anomalies in the North Pacific for observations (Fig. 6a–c) and for the different KCM ensembles (Fig. 6d–o). Additionally we show the wave-activity flux as vectors in Fig. 6 as an indication of the propagation features of quasi-stationary Rossby waves. The SLP response shows clear asymmetries, as it has a much stronger amplitude during EP El Niño than during CP El Niño, and the weakest amplitude during La Niña. The overall structure is best captured in the AMIP-type runs (Fig. 6d–f), especially for EP and CP El Niño. From SMALL to LARGE the SLP anomaly pattern in the North Pacific is located further westward, consistent with the westward shift of the convection in the tropical Pacific (Fig. 5). The elongated structure of the SLP anomaly in the CP El Niño and La Niña cases is not well captured in all three sub-ensembles. The quasi-stationary Rossby waves as shown by the wave-activity flux are consistent with the different positions of the SLP response. Further, the spatial asymmetry between the three event types decreases from SMALL to LARGE. Overall, La Niña anomalies seem to be on first view too strong in the model, underlining the stronger symmetry between El Niño and La Niña in the model as compared to observations. But as we show later, there are large uncertainties in the amplitudes, due to short observational records. But part of the underestimated asymmetry may be due to a biased representation of the differing seasonality between El Niño and La Niña in the North Pacific, where La Niña anomalies tend to weaken earlier, i.e., in February, than El Niño anomalies, which persist into March (Jiménez-Esteve and Domeisen 2018). This seasonality tends to be poorly

represented in models, as e.g., shown for CMIP5 models (Ayarzagüena et al. 2018).

For precipitation, EP El Niño exhibits the strongest observed precipitation anomaly over California (0.7 mm/day, Fig. 7a). CP El Niño events have the strongest precipitation response over the ocean and only lead to a small increase in precipitation in Southern California and dryness further north, while La Niña exhibits drying in Southern California. The precipitation response during ENSO events is overall well represented in the AMIP-type run, but a bit stronger over California (1.1 mm/day). The strongest difference to observations during La Niña is the too strong dry response off the coast and a north–south dipole along the west coast. Thus in AMIP-type experiments La Niña again exhibits a pattern that is almost exactly opposite to CP El Niño, unlike in observations. The coupled models first of all show only small differences in the shape and amplitude between the three event types. For EP El Niño the precipitation response is best represented in the SMALL SST bias sub-ensemble, both in terms of the magnitude and location of the precipitation (0.6 mm/day over California). With larger SST biases the model fails to reproduce the increased precipitation over California during EP El Niños, as the rainfall anomaly extends westward and therefore weakens considerably over California (0.3 mm/day in MEDIUM and 0.0 mm/day in LARGE), while a strong opposite-signed anomaly develops along the northern part of the coast. But due to a too linear precipitation response the model overestimates the increased precipitation over California during CP El Niño events in the SMALL sub-ensemble. In summary, the AMIP-type experiments best reproduce the teleconnection to California, while the sub-ensemble with the LARGE cold SST bias has considerable problems to simulate the observed location and asymmetry between the different types of ENSO.

To visualize the asymmetries in pattern and amplitude between EP El Niño, CP El Niño and La Niña and how they relate in the different KCM sub-ensembles, we show the center and amplitude of the patterns from Figs. 4, 5, 6 and 7 in Fig. 8. In order to obtain a measure to estimate if the modeled results are different from the observations we show an estimate of the uncertainties in the model experiments in Fig. 8. These uncertainties are estimated by a bootstrapping approach, where we subsample the model data into subsamples of the size of observations, similar to Garfinkel et al. (2018). This gives us an estimate if the observed values lie within the spread of our model results. Between the center of SST and the center of OLR there seems to be no clear linear or nonlinear relationship (Fig. 8a), as the center of OLR is quite different in the sub-ensembles, even though they have the same center of SST. This suggests that the different mean state positions of the rising branch of the Walker Circulation have a considerable influence on the location of the OLR response during ENSO events,

ENSO Composites of OLR in Obs and KCM



◀**Fig. 5** Same as Fig. 4, but here for OLR and additionally the KCM AMIP-type experiments are shown. The number in the header of each figure is the number of months, the amplitude of OLR and center of OLR along the equator between 5°S and 5°N, respectively and all figures are normalized by the corresponding center of heat amplitude of SST

as described in Bayr et al. (2018a). In Fig. 8b, c there is a nonlinear relationship between the center of OLR and the center of SLP and precipitation, i.e. the center of SLP and precipitation is determined by the center of OLR, as suggested by Ding et al. (2017). Further these figures visualize the spatial asymmetries between EP El Niño, CP El Niño and La Niña, which are quite substantial in observations, but underestimated in the KCM experiments. This asymmetry is most strongly underestimated in the LARGE SST bias sub-ensemble, which has nearly the same center of OLR, SLP and precipitation for all three ENSO flavors. The asymmetry increases with reduced SST bias, so that it is the largest in the AMIP-type experiments. For the amplitude of SST, OLR, SLP and precipitation the observations again show a large difference between ENSO flavors (Fig. 8d–f), which is to a good extent reproduced by the AMIP-type experiments. The coupled model fails to reproduce this difference, and especially the EP El Niño event is much too similar to the other two, which may be related to the strong underestimation of the SST warming close to the South American coast. A recent study of Lee et al. (2018) found that this far eastern warming is important for the asymmetrical teleconnection to the North Pacific during EP El Niño events. Finally we note that the uncertainty in the location and amplitude is quite large, in particular for the SLP and precipitation response, as indicated by the error bars in Fig. 8. This implies that the uncertainty in the observations is also large due to the limited sample size. Nevertheless, the observed location and amplitude are in most cases clearly distinct from the results of the coupled model, while the AMIP-type experiments agree well in most aspects with the observations.

To underline that the equatorial SST bias influences the location and strength of the ENSO teleconnection to the North Pacific, we now compare the individual experiments. As shown above the coupled KCM experiments exhibit a relationship of ENSO dynamics and ENSO teleconnections that is too linear. We therefore here consider all ENSO events together and do not separate them into EP El Niños, CP El Niños and La Niñas for a better overview. Figure 9a–c shows a very strong correlation between the SST bias in Niño4 and the location of the OLR, SLP and precipitation response of 0.96, 0.81 and 0.83, respectively. Thus KCM experiments with a larger SST bias tend to have a convective response in the tropics that is located too far to the west, which is related to a SLP and precipitation response that is shifted westward. There is also a very strong correlation

of -0.91 between the SST bias and the OLR amplitude (Fig. 9d), which can be explained by the stronger descending motion in the Niño4 region in models with a large SST bias (Fig. 2b), which weakens the ENSO feedbacks (Bayr et al. 2018a). The amplitude of SLP and precipitation also show a significant correlation of -0.51 and 0.44 with the SST bias, respectively (Fig. 9e, f), which can be related to the different strengths of the tropical convection forcing as shown in Fig. 9d.

As already indicated in Fig. 8, the asymmetry is in general underestimated in the coupled KCM experiments, but less in the SMALL sub-ensemble than in the LARGE sub-ensemble. To further analyze this, we have a look at the asymmetry between El Niño and La Niña at the centers of OLR, SLP and precipitation in the individual KCM experiments. For simplification we do not separate into EP and CP El Niños, as it can be seen in Fig. 8 that KCM strongly underestimates this asymmetry. Figure 10a shows that the asymmetry of the center of OLR between El Niño and La Niña is larger in the experiments with a smaller SST bias, with a quite strong correlation of 0.78. This can be explained by the stronger nonlinearity in ENSO dynamics in models with a weaker SST bias (Kim and Cai 2014; Bayr et al. 2018a). The stronger asymmetry in OLR results in a stronger asymmetry in the SLP and precipitation response in experiments with a weaker SST bias (Fig. 10b, c), with a significant correlation of 0.58 and 0.40, respectively. Interestingly, the sign of the asymmetry in SLP in observations is here different from most KCM experiments: In observations the center of SLP during La Niña tends to be located further eastward than during El Niño, while this is opposite in most KCM simulations (see also Fig. 6). The AMIP-type model also exhibits the opposite asymmetry than observations, indicating a problem of the atmospheric model to simulate a realistic SLP asymmetry or an uncertainty in the asymmetry of the observations.

6 CMIP5

Next it is investigated if a similar relationship can be found between the equatorial SST bias and the location of ENSO teleconnections in the CMIP5 models. First of all we have to note that the CMIP5 models have an overall weaker equatorial SST bias (Fig. 11a), but a similar spread (Fig. 11b) in comparison to the KCM (Fig. 2b). The CMIP5 models also show a significant correlation of 0.68 and -0.67 between the equatorial SST bias and the location of the shift from ascending to descending or convection strength in Niño4, respectively, but with a weaker correlation than in the KCM (0.96 and -0.97). As described in detail in Bayr et al. (2018a), the equatorial SST bias also hampers the atmospheric feedbacks in the CMIP5 models (Fig. 12b), as both

ENSO Composites of SLP in Obs and KCM

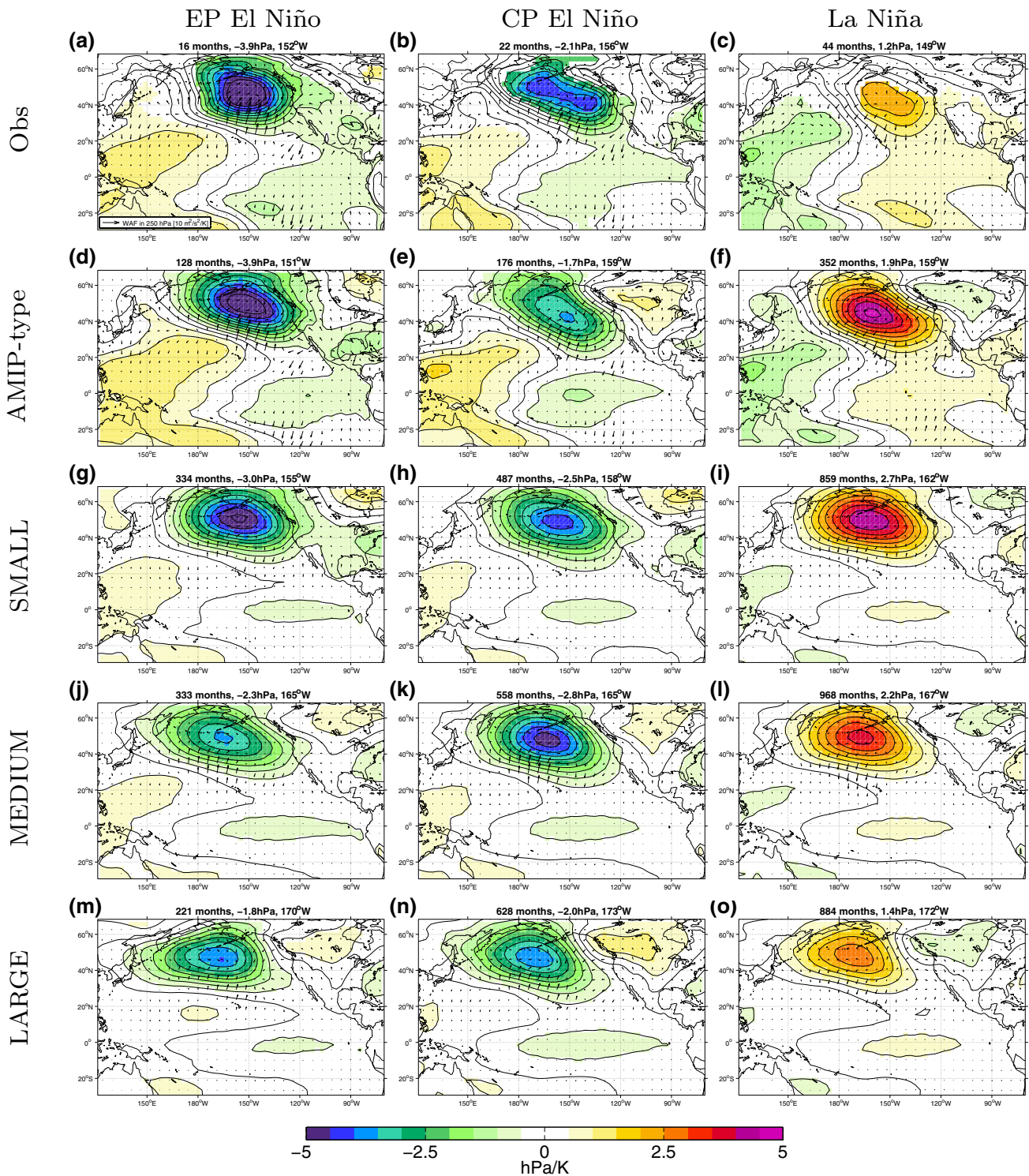


Fig. 6 Same as Fig. 5, but here for SLP. Additionally the composite of wave-activity flux anomalies is shown as vectors. The number in the header of each figure is the number of months, the amplitude and

the center of the SLP response between 30°N and 70°N, respectively and all figures are normalized by the corresponding center of heat amplitude of SST

ENSO Composites of Precip in Obs and KCM

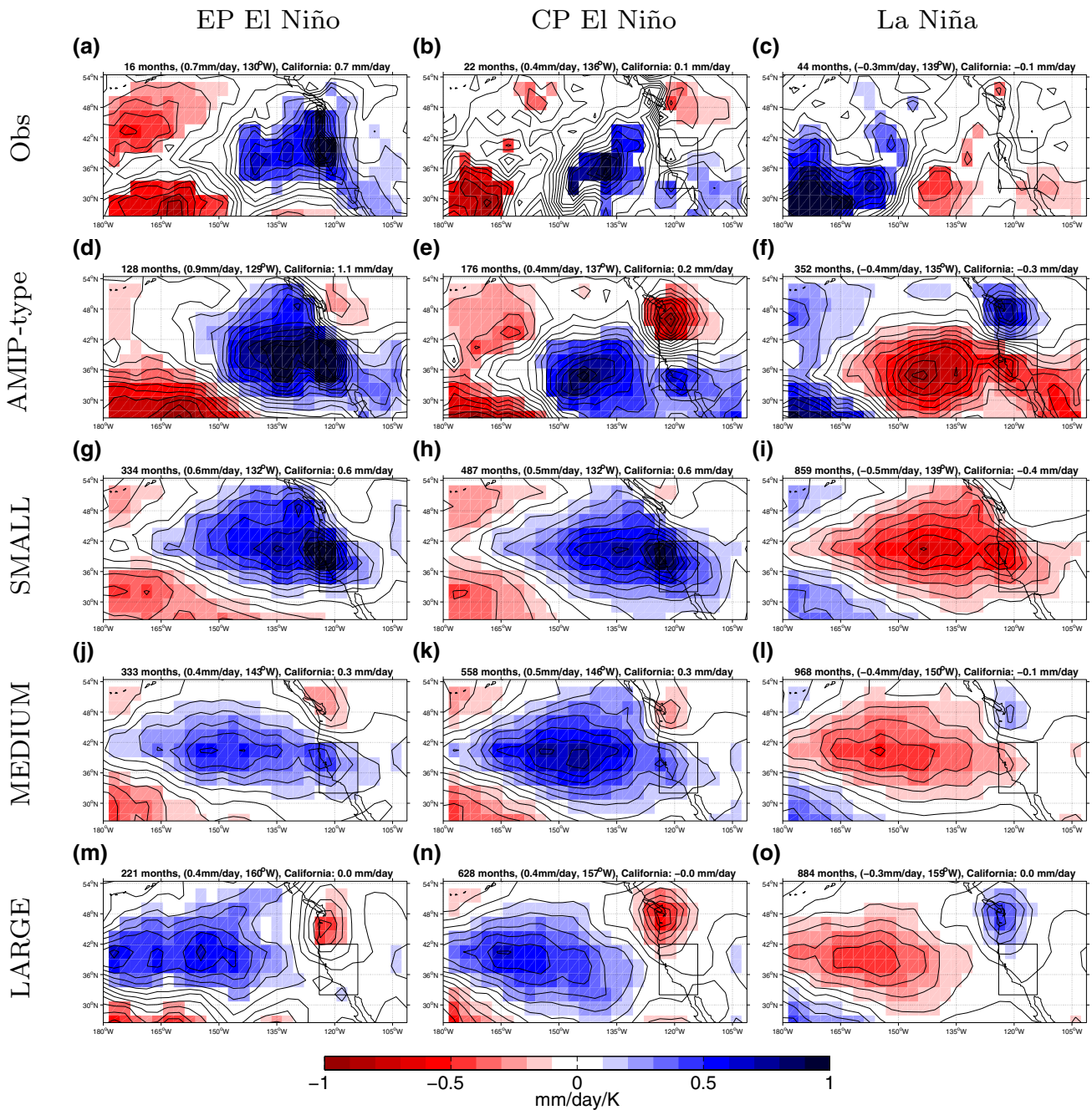


Fig. 7 Same as Fig. 5, but here for precipitation. The number in the header of each figure is the number of months, the amplitude and center of precipitation between 30°N and 45°N and the precipitation response over the region 114°W–124°W, 32°N–42°N as marked with

the black box (which is roughly California), respectively and all figures are normalized by the corresponding center of heat amplitude of SST

are also strongly linearly related to each other and underestimated in the models (Fig. 12a).

Looking at all types of ENSO events together in the individual CMIP5 models, a significant correlation of 0.47,

0.51 and 0.48 between the SST bias and the center of the OLR, SLP and precipitation, respectively can be found (Fig. 13a–c), i.e., the models with a larger SST bias also tend to simulate the equatorial convection, the North Pacific

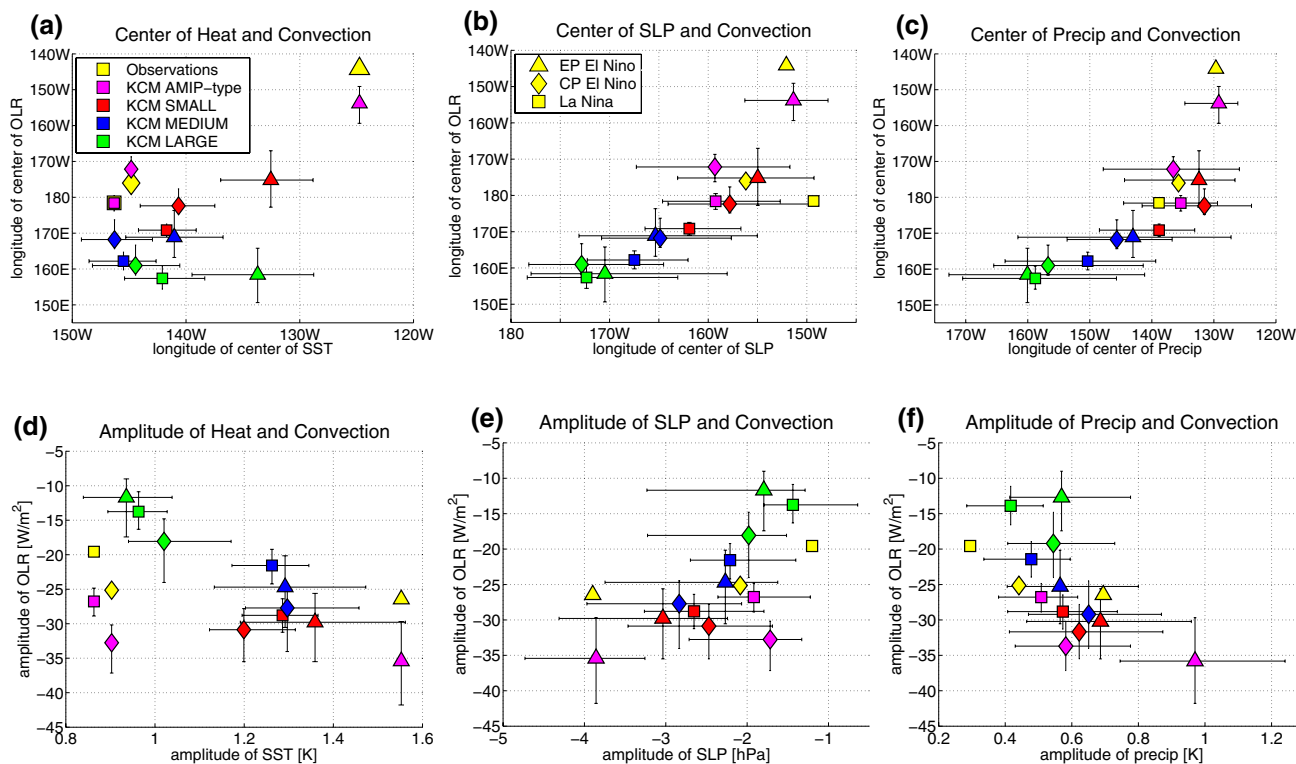


Fig. 8 For EP El Niño, CP El Niño and La Niña events in Observations/Reanalysis data, KCM AMIP-type experiments and KCM with SMALL, MEDIUM and LARGE cold SST bias in **a** longitude of the amplitude weighted center of SSTa along the equator (5°S – 5°N) on the x-axis vs. the longitude of the amplitude weighted center of OLR along the equator on y-axis; **b** same as **a** but here on the x-axis the longitude of the amplitude weighted center of SLP anomalies between 30°N and 70°N ; **c** same as **a**) but here on x-axis the center of precipitation in the region 30°N – 45°N ; **d** the SSTa amplitude aver-

aged along the equator (5°S – 5°N) on the x-axis vs. the OLR amplitude averaged along the equator on the y-axis; **e** same as **d** but here on the x-axis the amplitude of SLP pattern in the region 30°N and 70°N ; **f** same as **d** but here on x-axis the amplitude of precipitation in the region 30°N – 45°N . The errorbars mark the spread (with a 90% confidence level tested with a bootstrapping approach) that the modeled values would have, if the sample size would be as small as in observations. The amplitude of La Niña events is multiplied by -1 for a better comparison

SLP response and the subtropical precipitation response further westward. For the amplitude the CMIP5 models show a significant correlation of -0.55 between the OLR amplitude and the SST bias, but an insignificant correlation for SLP and precipitation (Fig. 13d–f).

For the asymmetry between El Niño and La Niña, CMIP5 models show a weak but significant correlation of 0.34 between the SST bias and the asymmetry in OLR (Fig. 14a). Further, the CMIP5 models show a strong correlation of 0.68 and 0.50 between the asymmetry of OLR and the asymmetry of SLP and precipitation, respectively (Fig. 14b, c), underlining that the asymmetry of OLR is important for the asymmetry in SLP and precipitation. However, similar to the KCM most of the CMIP5 models simulate the SLP center further west for El Niño as compared to La Niña, while in observations it is the other way around. Therefore these models have a different sign in asymmetry in SLP as compared to the observations, indicating a more general problem

in the models in simulating the correct SLP asymmetry or an uncertainty in the asymmetry in the observations.

Finally we have to note that in CMIP5 most of the correlations shown here are weaker than in the KCM. This is not surprising, as the CMIP5 models differ in many more aspects than the KCM ensemble. This results in more diverse relationship of the equatorial SST bias and the rising branch of the Pacific Walker Circulation as shown in Fig. 11b, or more diverse response pattern than in the KCM (e.g. pattern correlation of OLR composite pattern between the individual models and ensemble mean pattern is 0.82 ± 0.23 in CMIP5 and 0.95 ± 0.04 in KCM). Therefore the CHI longitude may not be as comparable and representative in the CMIP5 models as in KCM. Nevertheless the results underline that the equatorial SST bias hampers the simulation of ENSO teleconnections to the North Pacific and California in CMIP5 simulations.

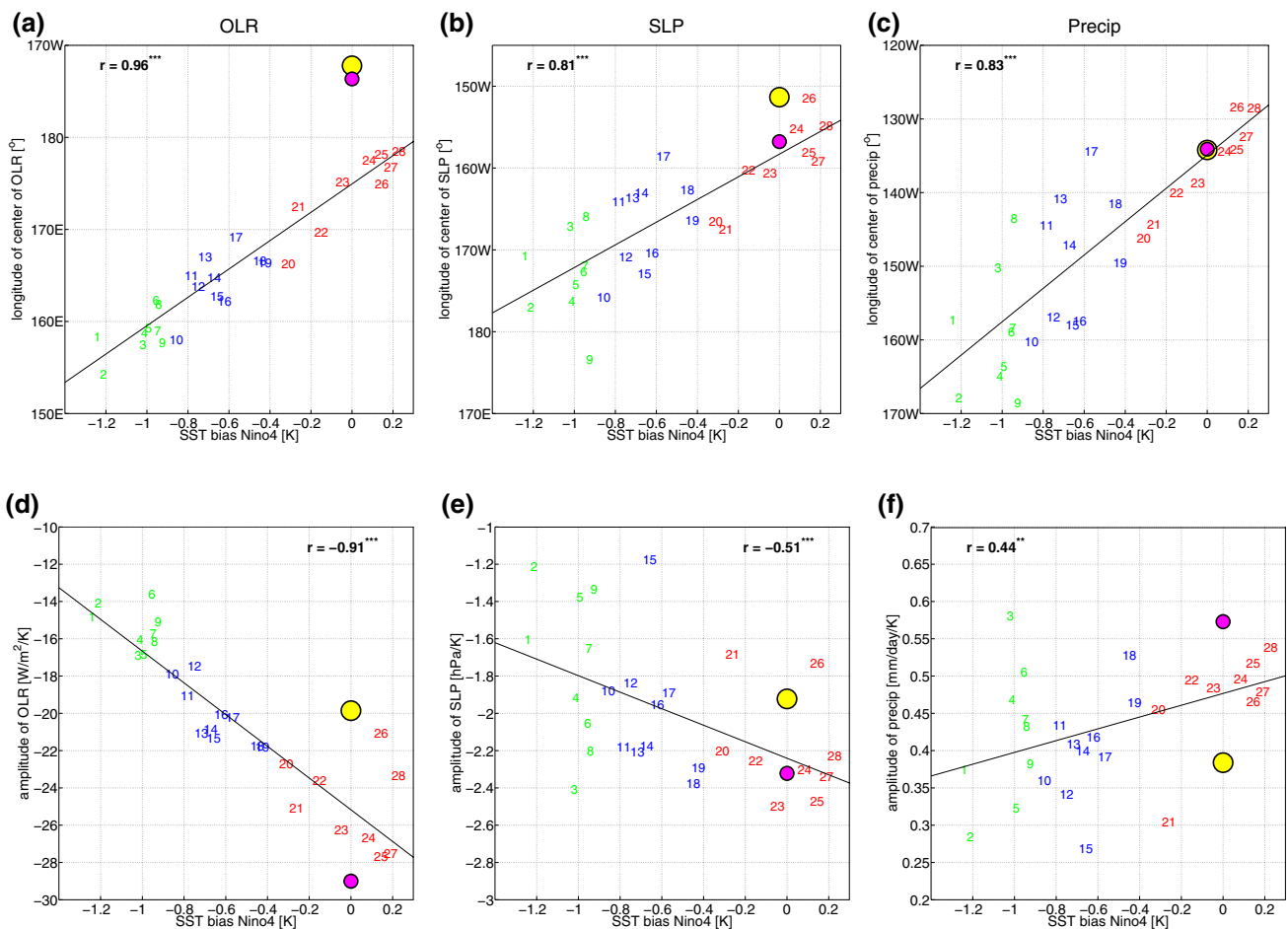


Fig. 9 For Reanalysis data (yellow circle), KCM AMIP-type experiments (margenta circle) and the individual KCM experiments, in **a** the SST bias in Niño4 on the x-axis vs. the longitude of the amplitude weighted center of OLR anomalies along the equator for all El Niño and La Niña events on y-axis; **b** same as **a** but here on the y-axis for the longitude of amplitude weighted center of SLP between 30°N and 70°N; **c** same as **a** but here on the y-axis for the center of precipitation between 30°N and 45°N; **d** same as **a** but here on the y-axis the OLR amplitude of all ENSO events averaged along the equator, i.e.

the average over all El Niño and La Niña events, after multiplying La Niña events by -1 ; **e** same as **d** but here on the y-axis the amplitude of SLP between 30°N and 70°N; **f** same as **d** but here on the y-axis the amplitude of precipitation between 30°N and 45°N; the colors of the numbers indicate the three sub-ensembles with LARGE (green), MEDIUM (blue) and SMALL (red) cold SST bias. One, two or three stars behind the correlation value indicates that the correlation is significant on a 90%, 95% or 99% confidence level, respectively

7 Summary and discussion

We investigated the influence of the equatorial Pacific SST bias on ENSO teleconnections to the North Pacific, with a focus on California. We have shown that the effects of the equatorial Pacific cold SST bias are not restricted to the tropics: The bias has a substantial influence on how ENSO teleconnections to the North Pacific are simulated. While AMIP-type simulations are able to reproduce most aspects of the observed teleconnection to the North Pacific and California, coupled climate models with an equatorial cold SST bias tend to exhibit a westward shift in the equatorial convective response that in turn leads to a westward shift in the SLP response in the North Pacific and the precipitation response in the subtropics. The bias in the tropical Pacific

thereby leads to a significant underestimation of the precipitation anomaly associated with ENSO over California. This relationship has here been shown in a perturbed physics ensemble of the KCM as well as in a CMIP5 multi-model ensemble.

The teleconnections arising from La Niña are shown to be similar but opposite in sign to the ones arising from CP El Niño. Furthermore, this study also confirms the results of Frauen et al. (2014) that teleconnections between EP and CP El Niño may need to be considered separately, although they may occur on a continuum. In particular, EP El Niño exhibits hints of nonlinearity for the longitudinal response of SLP in the North Pacific and precipitation over California to the longitude of the OLR anomalies along the equator, as well as for the amplitude of the precipitation response to

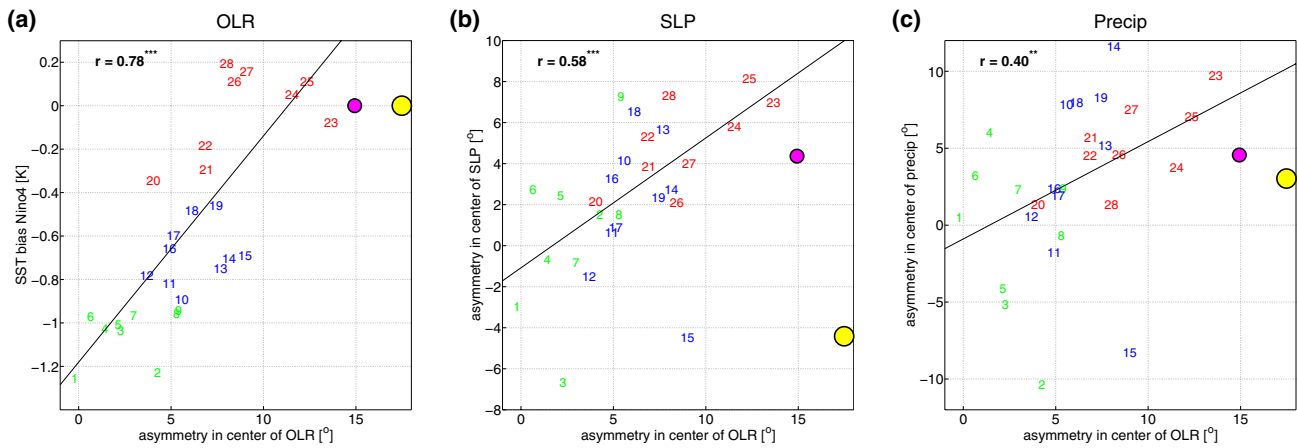


Fig. 10 For reanalysis data (yellow circle), KCM AMIP-type experiments (magenta circle) and the individual KCM experiments, in **a** the SST bias in Niño4 on the x-axis vs. asymmetry between El Niño and La Niña in the longitude of center of OLR anomalies along the equator on y-axis; positive values indicate a more eastern center during El Niño than during La Niña; **b** same as **a** but here on the y-axis the asymmetry between El Niño and La Niña in the center of SLP

between 30°N and 70°N; **c** same as **a** but here on the y-axis the asymmetry between El Niño and La Niña in the center of precipitation between 30°N and 45°N; the colors of the numbers indicate the three sub-ensembles with LARGE (green), MEDIUM (blue) and SMALL (red) cold SST bias. One, two or three stars behind the correlation value indicates that the correlation is significant on a 90%, 95% or 99% confidence level, respectively

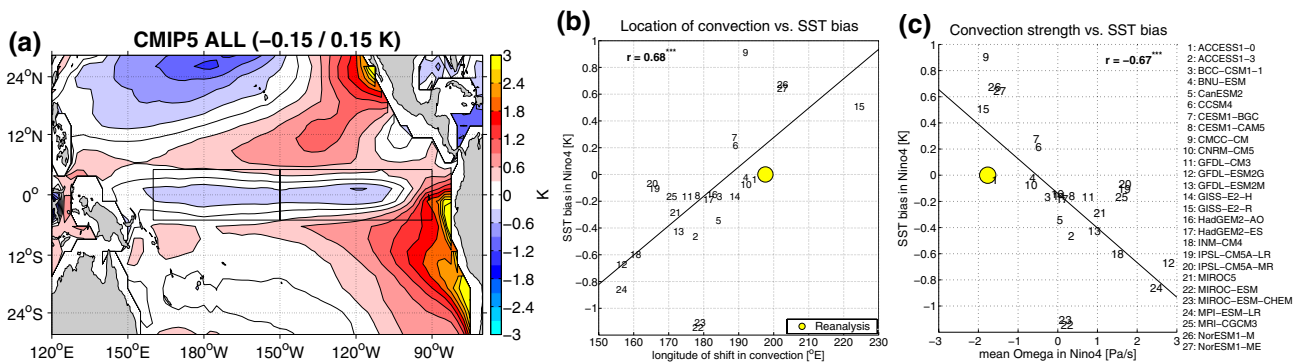
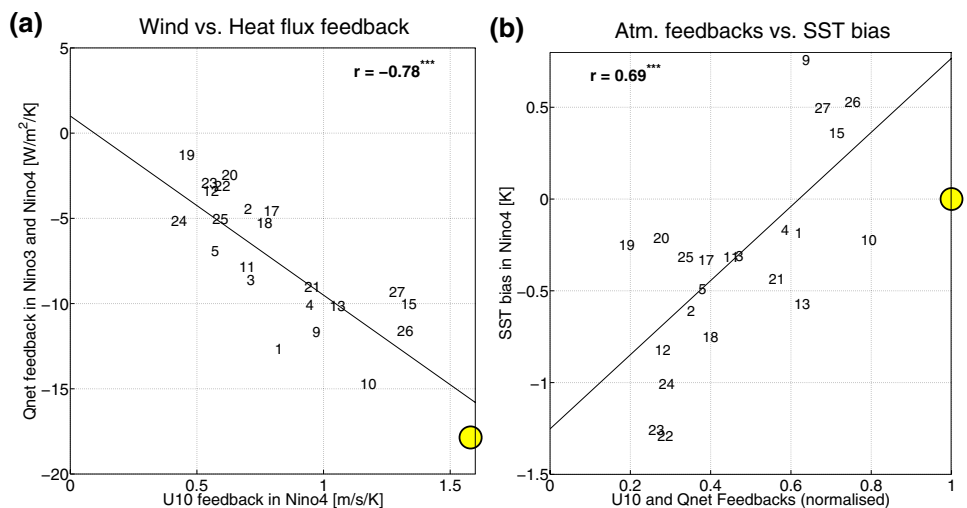


Fig. 11 a Tropical Pacific SST bias of the CMIP5 ensemble (area mean SST subtracted from each data set before calculating the SST bias); **b**, **c** same as Fig. 2b, c, but here for the CMIP5 models

Fig. 12 Same as Fig. 3, but here for the CMIP5 models



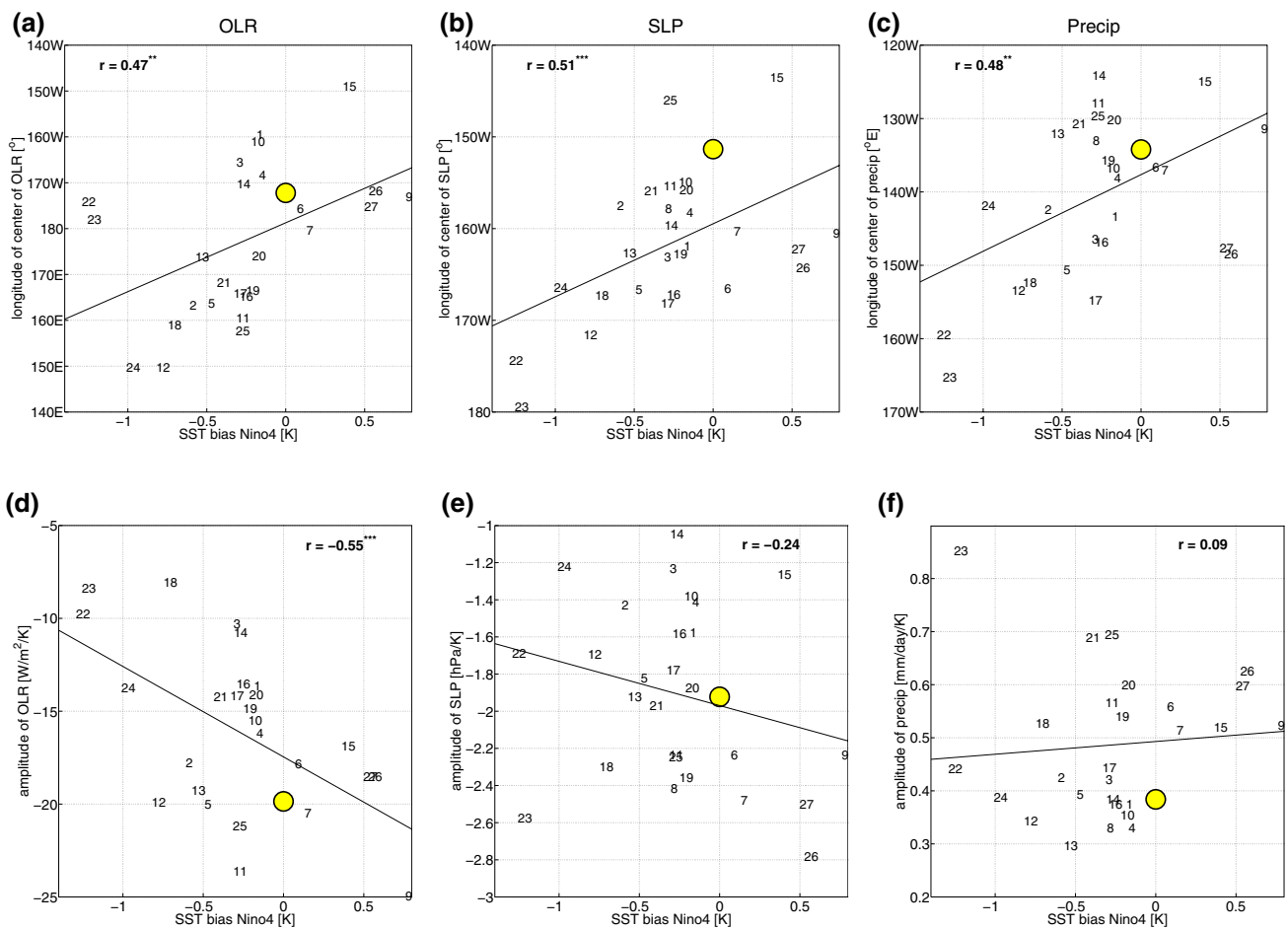


Fig. 13 Same as Fig. 9, but here for CMIP5 models

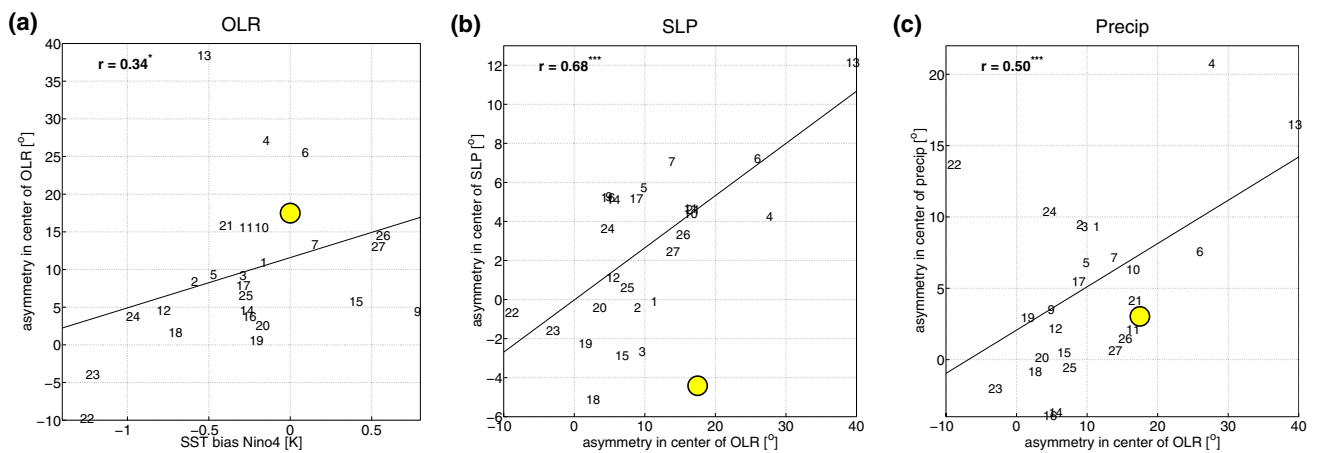


Fig. 14 Same as Fig. 10, but here for CMIP5 models

the amplitude of OLR anomalies. The nonlinearity in ENSO teleconnection can partly be explained by a nonlinear atmospheric response to the difference in amplitude of weak and strong El Niño events (Jiménez-Esteve and Domeisen 2019).

Further, the deviations from linear behavior for EP El Niño is consistent with Frauen et al. (2014), while CP El Niño exhibits more linear behavior, consistent with Zhang et al. (2018b).

Due to the limited number of ENSO events in the observational record and due to large internal atmospheric variability caused by e.g. the phase of the Pacific Decadal Oscillation, much longer observations are needed to gain more confidence about the true nature of ENSO teleconnections to the North Pacific and its asymmetries (Deser et al. 2017, 2018; Garfinkel et al. 2018; Domeisen et al. 2019). Therefore it is difficult to determine if the asymmetries of ENSO teleconnections to the North Pacific are well captured in climate models in comparison to observations. But our results clearly show that the SST biases hamper the simulated ENSO teleconnection to the North Pacific, as the AMIP-type experiments are closest to the observed ENSO teleconnection. Especially the asymmetry between EP and CP El Niño is well represented by the AMIP-type experiments, while all coupled KCM experiments fail to reproduce this asymmetry. The asymmetry between El Niño and La Niña is in general poorly represented in current climate models, but tends to be better represented in climate models with weak equatorial SST bias. This can be explained by the stronger ENSO atmospheric and oceanic feedbacks in climate models with a smaller SST bias, as stronger atmospheric and oceanic feedbacks improve the simulated ENSO diversity (Kim and Cai 2014; Bayr et al. 2018a, b).

The equatorial cold SST bias is a common problem in current climate models and its causes are still under debate (Davey et al. 2002; Guilyardi et al. 2009; Vanni ere et al. 2013; Bayr et al. 2018a). Due to the equatorial cold SST bias the atmosphere is in a La Ni a-like mean state, with a westward shifted position of the rising branch of the Walker Circulation that leads to a westward shift in the equatorial convective response during ENSO events. In the CMIP5 models the sensitivity of the atmosphere to the SST bias differs more considerably among the models (Fig. 11b) as compared to the KCM model ensemble (Fig. 2b). This may explain the higher robustness of the results in the perturbed physics ensemble of the KCM in comparison to the CMIP5 ensemble.

A difference between the KCM and the CMIP5 ensemble is the sign of the SST bias in the North Pacific, which may have an influence on the ENSO teleconnection to the North Pacific. Further it is important to note that the changed convection parameters in the perturbed physics ensemble of KCM may also have an influence on the mean circulation in the North Pacific, which may itself have an effect on ENSO teleconnections, as described e.g. in Lu et al. (2008). But as we stay with the parameters in the range of physical uncertainties, as suggested by Mauritsen et al. (2012), this effect should not be large. Indeed, the mean midlatitude circulation, such as the storm tracks, does not significantly differ in the individual experiments. Finally, a similar relation between ENSO teleconnection and the equatorial SST bias in both the KCM and CMIP5 simulations indicates that the

equatorial Pacific SST bias seems to play an important role for the location of the ENSO teleconnection to the North Pacific.

The findings from this study may have major consequences on how ENSO teleconnections are simulated and forecasted. ENSO is used for the seasonal prediction of a variety of global remote impacts. As has been shown, a bias in the simulation of the tropical Pacific may crucially impact the ENSO teleconnection to California. This finding will have consequences for regions at a longer distance from the tropical Pacific that are affected by ENSO and that rely on ENSO for sub-seasonal to seasonal prediction, such as Australia (Chiew et al. 1998) and the North Atlantic and Europe (Br nnimann 2007; Domeisen et al. 2015; Butler et al. 2016; Dunstone et al. 2016). Further studies will have to show if the limitations arising from the equatorial SST bias are a reason for the opposing results between observational studies and model simulations for teleconnections to the Northern Hemisphere stratosphere, as e.g., shown in Butler and Polvani (2011), Garfinkel et al. (2012a) and Domeisen et al. (2019).

Acknowledgements The authors would like to thank the anonymous reviewers for their comments that helped to improve the manuscript. We acknowledge the World Climate Research Program’s Working Group on Coupled Modeling, the individual modeling groups of the Climate Model Intercomparison Project (CMIP5), NOAA and ECMWF for providing the data sets. The climate model integrations of the KCM and ECHAM5 were performed at the Computing Centre of Kiel University and the Northern German Supercomputing Alliance (HLRN). This work is supported by the SFB grant 754 “Climate-Biochemistry Interactions in the tropical Ocean”, the Swiss National Science Foundation through Grant no. PP00P2_170523, and the German Ministry of Education and Research (BMBF) through Grant SACUS (03G0837A). The authors would like to thank Mojib Latif, Dietmar Dommeng et and Gereon Gollan for helpful discussions.

References

- Ashok K, Behera SK, Rao SA, Weng H, Yamagata T (2007) El Ni o Modoki and its possible teleconnection. *J Geophys Res* 112. <https://doi.org/10.1029/2006JC003798>
- Ayarzag uena B, Ineson S, Dunstone NJ, Baldwin MP, Scaife AA (2018) Intraseasonal effects of El Ni o-Southern Oscillation on North Atlantic climate. *J Clim* 31:8861–8873. <https://doi.org/10.1175/JCLI-D-18-0097.1>
- Banzon V, Smith TM, Chin TM, Liu C, Hankins W (2016) A long-term record of blended satellite and in situ sea-surface temperature for climate monitoring, modeling and environmental studies. *Earth Syst Sci Data* 8(1):165–176. <https://doi.org/10.5194/essd-8-165-2016>
- Barnston AG, Livezey RE (1987) Classification, seasonality and persistence of low-frequency atmospheric circulation patterns. *Mon Weather Rev* 115:1083–1126
- Bayr T, Dommeng et D (2013) The tropospheric land–sea warming contrast as the driver of tropical sea level pressure changes. *J Clim* 26(4):1387–1402. <https://doi.org/10.1175/JCLI-D-11-00731.1>

- Bayr T, Dommenges D, Martin T, Power SB (2014) The eastward shift of the Walker Circulation in response to global warming and its relationship to ENSO variability. *Clim Dyn* 43(9):2747–2763. <https://doi.org/10.1007/s00382-014-2091-y>
- Bayr T, Latif M, Dommenges D, Wengel C, Harlaß J, Park W (2018a) Mean-state dependence of ENSO atmospheric feedbacks in climate models. *Clim Dyn* 50(9–10):3171–3194. <https://doi.org/10.1007/s00382-017-3799-2>
- Bayr T, Wengel C, Latif M, Dommenges D, Lübbecke J, Park W (2018b) Error compensation of ENSO atmospheric feedbacks in climate models and its influence on simulated ENSO dynamics. *Clim Dyn*. <https://doi.org/10.1007/s00382-018-4575-7>
- Bellenger H, Guilyardi E, Leloup J, Lengaigne M, Vialard J (2014) ENSO representation in climate models: from CMIP3 to CMIP5. *Clim Dyn* 42(7–8):1999–2018. <https://doi.org/10.1007/s00382-013-1783-z>
- Brönnimann S (2007) Impact of El Niño-Southern Oscillation on European climate. *Rev Geophys* 45(3):1–28
- Butler AH, Polvani LM (2011) El Niño, La Niña, and stratospheric sudden warmings: a reevaluation in light of the observational record. *Geophys Res Lett* 38(13):L13–807. <https://doi.org/10.1029/2011GL048084>
- Butler AH, Arribas A, Athanassiadou M, Baehr J, Calvo N, Charlton-Perez A, Déqué M, Domeisen DIV, Fröhlich K, Hendon H, Imada Y, Ishii M, Iza M, Karpechko AY, Kumar A, MacLachlan C, Merryfield WJ, Müller WA, O'Neill A, Scaife AA, Scinocca J, Sigmund M, Stockdale TN, Yasuda T (2016) The Climate-system Historical Forecast Project: do stratosphere-resolving models make better seasonal climate predictions in boreal winter? *Q J R Meteorol Soc* 142(696):1413–1427
- Capotondi A, Wittenberg AT, Newman M, Di Lorenzo E, Yu JY, Braconnot P, Cole J, Dewitte B, Giese B, Guilyardi E, Jin FF, Karnauskas K, Kirtman B, Lee T, Schneider N, Xue Y, Yeh SW (2015) Understanding ENSO diversity. *Bull Am Meteorol Soc* 96(6):921–938
- Cayan DR, Redmond KT, Riddle LG (1999) ENSO and hydrologic extremes in the Western United States: EBSCOhost. *J Clim* 12:2881–2893
- Chen Z, Gan B, Wu L, Jia F (2018) Pacific-North American teleconnection and North Pacific Oscillation: historical simulation and future projection in CMIP5 models. *Clim Dyn* 50(11–12):4379–4403. <https://doi.org/10.1007/s00382-017-3881-9>
- Chiew FHS, Piechota TC, Dracup JA, McMahon TA (1998) El Niño/Southern Oscillation and Australian rainfall, streamflow and drought: links and potential for forecasting. *J Hydrol* 204(1–4):138–149
- Chiodi AM, Harrison DE (2013) El Niño impacts on seasonal US atmospheric circulation, temperature, and precipitation anomalies: the OLR-event perspective*. *J Clim* 26(3):822–837
- Chiodi AM, Harrison DE (2015) Global seasonal precipitation anomalies robustly associated with El Niño and La Niña events—an OLR perspective*. *J Clim* 28(15):6133–6159
- Davey M, Huddleston M, Sperber K, Braconnot P, Bryan F, Chen D, Colman R, Cooper C, Cubasch U, Delecluse P, DeWitt D, Fairhead L, Flato G, Gordon C, Hogan T, Ji M, Kimoto M, Kitoh A, Knutson T, Latif M, Le Treut H, Li T, Manabe S, Mechoso C, Meehl G, Power S, Roeckner E, Terray L, Vintzileos A, Voss R, Wang B, Washington W, Yoshikawa I, Yu J, Yukimoto S, Zebiak S (2002) STOIC: a study of coupled model climatology and variability in tropical ocean regions. *Clim Dyn* 18(5):403–420. <https://doi.org/10.1007/s00382-001-0188-6>
- Dee D, Uppala S, Simmons A, Berrisford P, Poli P, Kobayashi S, Andrae U, Balmaseda M, Balsamo G, Bauer P, Bechtold P, Beljaars A, Berg L, Bidlot J, Bormann N, Delsol C, Dragani R, Fuentes M, Geer A, Haimberger L, Healy S, Hersbach H, Holm E, Isaksen L, Källberg P, Köhler M, Matricardi M, McNally A, Monge-Sanz B, Morcrette J, Park B, Peubey C, Rosnay Pd, Tavolato C, Thepaut J, Vitart F (2011) The ERA-Interim reanalysis: configuration and performance of the data assimilation system. *Q J Royal Met Soc* 137:553–597
- Deser C, Simpson IR, McKinnon KA, Phillips AS, Deser C, Simpson IR, McKinnon KA, Phillips AS (2017) The Northern Hemisphere extra-tropical atmospheric circulation response to ENSO: How well do we know it and how do we evaluate models accordingly? *J Clim*. <https://doi.org/10.1175/JCLI-D-16-0844.1>
- Deser C, Simpson IR, Phillips AS, McKinnon KA (2018) How well do we know ENSO's climate impacts over North America, and how do we evaluate models accordingly? *J Clim* 31(13):4991–5014. <https://doi.org/10.1175/JCLI-D-17-0783.1>
- Ding S, Chen W, Graf HF, Guo Y, Nath D (2017) Distinct winter patterns of tropical Pacific convection anomaly and the associated extratropical wave trains in the Northern Hemisphere. *Clim Dyn* 4(C11):1147
- Domeisen DIV, Butler AH, Fröhlich K, Bittner M, Müller WA, Baehr J (2015) Seasonal predictability over Europe arising from El Niño and stratospheric variability in the MPI-ESM seasonal prediction system. *J Clim* 28(1):256–271
- Domeisen DIV, Garfinkel CI, Butler AH (2019) The teleconnection of El Niño Southern Oscillation to the stratosphere. *Rev Geophys*. <https://doi.org/10.1029/2018RG000596>
- Dommenges D, Haase S, Bayr T, Frauen C (2014) Analysis of the Slab Ocean El Niño atmospheric feedbacks in observed and simulated ENSO dynamics. *Clim Dyn* 42(11–12):3187–3205
- Dong L, Leung LR, Song F, Lu J (2018) Roles of SST versus internal atmospheric variability in winter extreme precipitation variability along the US West Coast. *J Clim* 31(19):8039–8058. <https://doi.org/10.1175/JCLI-D-18-0062.1>
- Drews A, Greatbatch RJ, Ding H, Latif M, Park W (2015) The use of a flow field correction technique for alleviating the North Atlantic cold bias with application to the Kiel Climate Model. *Ocean Dyn* 65(8):1079–1093. <https://doi.org/10.1007/s10236-015-0853-7>
- Dunstone N, Smith D, Scaife A, Hermanson L, Eade R, Robinson N, Andrews M, Knight J (2016) Skilful predictions of the winter North Atlantic Oscillation 1 year ahead. *Nat Geosci* 9(11):809–814
- Frauen C, Dommenges D, Tyrrell N, Reznay M, Wales S (2014) Analysis of the nonlinearity of El Niño-Southern Oscillation teleconnections*. *J Clim* 27(16):6225–6244
- Garfinkel CI, Butler AH, Waugh DW, Hurwitz MM, Polvani LM (2012a) Why might stratospheric sudden warmings occur with similar frequency in El Niño and La Niña winters? *J Geophys Res Atmos* 117. <https://doi.org/10.1029/2012JD017777>
- Garfinkel CI, Hurwitz MM, Waugh DW, Butler AH (2012b) Are the teleconnections of Central Pacific and Eastern Pacific El Niño distinct in boreal wintertime? *Clim Dyn* 41(7–8):1835–1852
- Garfinkel CI, Weinberger I, White IP, Oman LD, Aquila V, Lim YK (2018) The salience of nonlinearities in the boreal winter response to ENSO: North Pacific and North America. *Clim Dyn* 4(C11):1147
- Giese BS, Ray S (2011) El Niño variability in simple ocean data assimilation (SODA), 1871–2008. *J Geophys Res* 116:C02024. <https://doi.org/10.1029/2010JC006695>
- Gill AE (1980) Some simple solutions for heat-induced tropical circulation. *Q J R Meteorol Soc* 106(449):447–462. <https://doi.org/10.1002/qj.49710644905>
- Guan C, McPhaden MJ (2016) Ocean processes affecting the twenty-first-century shift in ENSO SST variability. *J Clim* 29(19):6861–6879
- Guilyardi E, Wittenberg A, Fedorov A, Collins M, Wang C, Capotondi A, van Oldenborgh GJ, Stockdale T (2009) Understanding El Niño in ocean-atmosphere general circulation models:

- progress and challenges. *Bull Am Meteorol Soc* 90(3):325–340. <https://doi.org/10.1175/2008BAMS2387.1>
- Harlaß J, Latif M, Park W (2015) Improving climate model simulation of tropical Atlantic sea surface temperature: the importance of enhanced vertical atmosphere model resolution. *Geophys Res Lett* 42(7):2401–2408. <https://doi.org/10.1002/2015GL063310>
- Hoell A, Hoerling M, Eischeid J, Wolter K, Dole R, Perlwitz J, Xu T, Cheng L (2016) Does El Niño intensity matter for California precipitation? *Geophys Res Lett* 43(2):819–825
- Hoskins BJ, Karoly D (1981) The steady linear response of a spherical atmosphere to thermal and orographic forcing. *J Atmos Sci* 38(06):1179–1196
- Hurwitz MM, Song IS, Oman LD, Newman PA, Molod AM, Frith SM, Nielsen JE (2011) Response of the Antarctic stratosphere to warm pool El Niño Events in the GEOS CCM. *Atmos Chem Phys* 11(18):9659–9669
- Jiménez-Esteve B, Domeisen DI (2019) Nonlinearity in the North Pacific atmospheric response to a linear ENSO forcing. *Geophys Res Lett*. <https://doi.org/10.1029/2018gl081226>
- Jiménez-Esteve B, Domeisen DIV (2018) The Tropospheric Pathway of the ENSO-North Atlantic Teleconnection. *J Clim*. <https://doi.org/10.1175/JCLI-D-17-0716.1>
- Johnson NC, Kosaka Y (2016) The impact of eastern equatorial Pacific convection on the diversity of boreal winter El Niño teleconnection patterns. *Clim Dyn* 47(12):3737–3765. <https://doi.org/10.1007/s00382-016-3039-1>
- Jong BT, Ting M, Seager R (2016) El Niño's impact on California precipitation: seasonality, regionality, and El Niño intensity. *Environ Res Lett* 11(5):054021
- Kao HY, Yu JY (2009) Contrasting Eastern-Pacific and Central-Pacific types of ENSO. *J Clim* 22(3):615–632. <https://doi.org/10.1175/2008JCLI2309.1>
- Kim WM, Cai W (2014) The importance of the eastward zonal current for generating extreme El Niño. *Clim Dyn* 42(11–12):3005–3014. <https://doi.org/10.1007/s00382-013-1792-y>
- Kug J-S, Ham Y-G (2011) Are there two types of La Nina? *Geophys Res Lett* 38:L16704. <https://doi.org/10.1029/2011GL048237>
- Kumar A, Chen M (2017) What is the variability in US west coast winter precipitation during strong El Niño events? *Clim Dyn* 49(7–8):2789–2802. <https://doi.org/10.1007/s00382-016-3485-9>
- Larkin NK, Harrison DE (2005) Global seasonal temperature and precipitation anomalies during El Niño autumn and winter. *Geophys Res Lett* 32. <https://doi.org/10.1029/2005GL022860>
- Latif M, Keenlyside NS (2009) El Niño/Southern Oscillation response to global warming. *PNAS* 106(49):20578–20583
- Leathers DJ, Palecki MA (1992) The Pacific/North American teleconnection pattern and United States climate. Part II: Temporal characteristics and index specification. *J Clim* 5(7):707–716
- Leathers DJ, Yarnal B, Palecki MA (1991) The Pacific/North American teleconnection pattern and United States climate. Part I: Regional temperature and precipitation associations. *J Clim* 4(5):517–528
- Lee SK, Lopez H, Chung ES, DiNezio P, Yeh SW, Wittenberg AT (2018) On the Fragile relationship between El Niño and California rainfall. *Geophys Res Lett* 45(2):907–915. <https://doi.org/10.1002/2017GL076197>
- Liebmann B, Smith CA (1996) Description of a complete (interpolated) outgoing longwave radiation dataset. *Bull Am Meteorol Society* 77(6):1275–1277
- Lloyd J, Guilyardi E, Weller H (2012) The role of atmosphere feedbacks during ENSO in the CMIP3 models. Part III: The shortwave flux feedback. *J Clim* 25(12):4275–4293. <https://doi.org/10.1175/JCLI-D-11-00178.1>
- Lu J, Chen G, Frierson DMW (2008) Response of the zonal mean atmospheric circulation to El Niño versus global warming. *J Clim* 21:5835–5851. <https://doi.org/10.1175/2008JCLI2200.1>
- MacDonald GM, Kremenetski KV, Hidalgo HG (2008) Southern California and the perfect drought: simultaneous prolonged drought in southern California and the Sacramento and Colorado River systems. *Q Int* 188(1):11–23
- Madec G (2008) NEMO ocean engine. *Note du Pole de modélisation* 27, Institut Pierre-Simon Laplace p 193
- Mauritsen T, Stevens B, Roeckner E, Crueger T, Esch M, Giorgetta M, Haak H, Jungclaus J, Klocke D, Matei D, Mikolajewicz U, Notz D, Pincus R, Schmidt H, Tomassini L (2012) Tuning the climate of a global model. *J Adv Model Earth Syst* 4(3) <https://doi.org/10.1029/2012MS000154>
- McPhaden MJ (2012) A 21st century shift in the relationship between ENSO SST and warm water volume anomalies. *Geophys Res Lett* 39(9)
- Mo KC, Higgins RW (1998) Tropical influences on California precipitation. *J Clim* 11(3):412–430
- Mo KC, Livezey RE (1986) Tropical-extratropical geopotential height teleconnections during the Northern Hemisphere Winter. *Mon Weather Rev* 114(12):2488–2515
- Paek H, Yu JY, Qian C (2017) Why were the 2015/2016 and 1997/1998 extreme El Niños different? *Geophys Res Lett* 44(4):1848–1856. <https://doi.org/10.1002/2016GL071515>
- Park W, Keenlyside N, Latif M, Ströh A, Redler R, Roeckner E, Madec G (2009) Tropical Pacific climate and its response to global warming in the Kiel Climate model. *J Clim* 22(1):71–92
- Piechota TC, Dracup JA (1996) Drought and regional hydrologic variations in the United States: associations with the El Niño-Southern Oscillation. *Water Resour Res* 32(5):1359–1373
- Piechota TC, Dracup JA, Fovell RG (1997) Western US streamflow and atmospheric circulation patterns during El Niño-Southern Oscillation. *J Hydrol* 201(1–4):249–271
- Rasmusson EM, Wallace JM (1983) Meteorological aspects of the El Niño/Southern Oscillation. *Science* 222:1195–1202
- Roeckner E, Bauml G, Bonventura L, Brokopf R, Esch M, Giorgetta M, Hagemann S, Kirchner I, Kornblueh L, Manzini E, Rhodin A, Schlese U, Schulzweida U, Tompkins A (2003) The atmospheric general circulation model ECHAM5. Part I: Model description. 349, Max Planck Institute for Meteorology, Hamburg, Germany
- Schonher T, Nicholson SE (1989) The relationship between California Rainfall and Enso Events. *J Clim* 2(11):1258–1269
- Seager R, Naik N, Ting M, Cane MA, Harnik N, Kushnir Y (2010) Adjustment of the atmospheric circulation to tropical Pacific SST anomalies: variability of transient eddy propagation in the Pacific-North America sector. *Q J R Meteorol Society* 136:277–296
- Siler N, Kosaka Y, Xie SP, Li X (2017) Tropical ocean contributions to California's surprisingly dry El Niño of 2015/16. *J Clim* 30(24):10,067–10,079. <https://doi.org/10.1175/JCLI-D-17-0177.1>
- Sun Y, Wang F, Sun DZ (2016) Weak ENSO asymmetry due to weak nonlinear air–sea interaction in CMIP5 climate models. *Adv Atmos Sci* 33(3):352–364. <https://doi.org/10.1007/s00376-015-5018-6>
- Takaya K, Nakamura H (2001) A formulation of a phase-independent wave-activity flux for stationary and migratory quasigeostrophic eddies on a zonally varying basic flow. *J Atmos Sci* 58:608–627. <https://doi.org/10.1109/27.659538>
- Taylor KE, Stouffer RJ, Ga Meehl (2012) An overview of CMIP5 and the experiment design. *Bull Am Meteorol Soc* 93(4):485–498. <https://doi.org/10.1175/BAMS-D-11-00094.1>
- Timmermann A, Si An, Js Kug, Ff Jin, Cai W, Cobb K, Lengaigne M, McPhaden MJ, Malte F, Stein K, Wittenberg AT, Ks Yun, Bayr T, Hc Chen, Chikamoto Y, Dewitte B, Dommenges D, Grothe P, Yg Ham, Hayashi M, Ineson S, Kang D, Kim W, Jy Lee, Li T, Jj Luo, Mgregor S, Power S, Rashid H, Hl Ren, Santoso A, Takahashi K, Todd A, Wang G, Wang G, Xie R, Yang Wh, Yeh W, Yoon J, Zeller E, Zhang X (2018) El Niño-Southern Oscillation Complexity. *Nature*. <https://doi.org/10.1038/s41586-018-0252-6>

- Tompkins AM (1997) On the relationship between tropical convection and sea surface temperature. *J Clim* 14:633–637
- Trenberth KE (1997) The definition of El Niño. *Bull Am Meteorol Society* 78(12):2771–2777
- Trenberth KE, Stepaniak DP (2001) Indices of El Niño evolution. *J Clim* 14(8):1697–1701
- Trenberth KE, Branstator GW, Karoly D, Kumar A, Lau NC, Ropelewski C (1998) Progress during TOGA in understanding and modeling global teleconnections associated with tropical sea surface temperatures. *J Geophys Res* 198103(C7):14291–14324
- Vannière B, Guilyardi E, Madec G, Doblas-Reyes FJ, Woolnough S (2013) Using seasonal hindcasts to understand the origin of the equatorial cold tongue bias in CGCMs and its impact on ENSO. *Clim Dyn* 40(3–4):963–981. <https://doi.org/10.1007/s00382-012-1429-6>
- Wallace JM, Gutzler DS (1981) Teleconnections in the geopotential height field during the northern hemisphere winter. *Mon Weather Rev* 109(4):784–812
- Wang S, Anichowski A, Tippett MK, Sobel AH (2017) Seasonal noise versus subseasonal signal: forecasts of California precipitation during the unusual winters of 2015–2016 and 2016–2017. *Geophys Res Lett* 44(18):9513–9520. <https://doi.org/10.1002/2017GL075052>
- Wang Z, Kuhlbrodt T, Meredith MP (2011) On the response of the Antarctic Circumpolar Current transport to climate change in coupled climate models. *J Geophys Res* 116(C8):C08–011. <https://doi.org/10.1029/2010JC006757>
- Wengel C, Latif M, Park W, Harlaß J, Bayr T (2018) Seasonal ENSO phase locking in the Kiel Climate Model: the importance of the equatorial cold sea surface temperature bias. *Clim Dyn* 50(3–4):901–919. <https://doi.org/10.1007/s00382-017-3648-3>
- Xie P, Arkin PA (1997) Global precipitation: a 17-year monthly analysis based on Gauge observations, satellite estimates, and numerical model outputs. *Bull Am Meteorol Soc* 78(11):2539–2558
- Yoon Jin-Ho, Leung L Ruby (2015) Assessing the relative influence of surface soil moisture and ENSO SST on precipitation predictability over the contiguous United States. *Geophys Res Lett* 42:5005–5013. <https://doi.org/10.1002/2015GL064139>
- Zhang T, Perlwitz J, Hoerling MP (2014) What is responsible for the strong observed asymmetry in teleconnections between El Niño and La Niña? *Geophys Res Lett* 41(3):1019–1025
- Zhang T, Hoerling MP, Wolter K, Eischeid J, Cheng L, Hoell A, Perlwitz J, Quan XW, Barsugli J (2018a) Predictability and prediction of Southern California rains during Strong El Niño Events: a focus on the failed 2016 winter rains. *J Clim* 31(2):555–574
- Zhang W, Wang Z, Stuecker MF, Turner AG, Jin FF, Geng X (2018b) Impact of ENSO longitudinal position on teleconnections to the NAO. *Clim Dyn* 15:2205–18

Publisher's Note Springer Nature remains neutral with regard to jurisdictional claims in published maps and institutional affiliations.